

Discovery of C₂₀-Diterpenoid Alkaloid Kobusine Derivatives Exhibiting Sub-G1 Inducing Activity

Koji Wada,^{*,§} Masuo Goto,[§] Hisano Tanaka, Megumi Mizukami, Yuji Suzuki, Kuo-Hsiung Lee, and Hiroshi Yamashita



Cite This: *ACS Omega* 2022, 7, 28173–28181



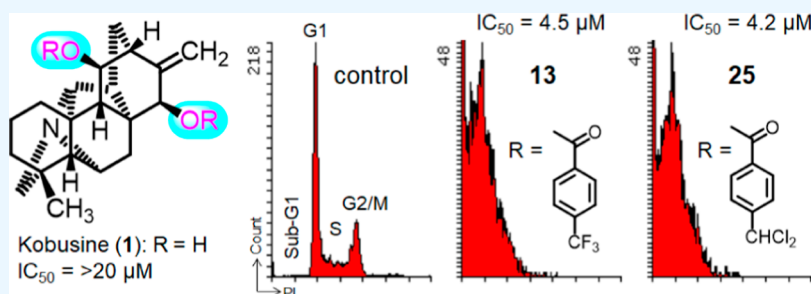
Read Online

ACCESS |

Metrics & More

Article Recommendations

Supporting Information



ABSTRACT: Although many diterpenoid alkaloids have been evaluated recently for antiproliferative activity against human cancer cell lines, little data have been offered relating to the antiproliferative effects of hetisine-type C₂₀-diterpenoid alkaloids, such as kobusine (1), likewise as their derivatives. A total of 43 novel diterpenoid alkaloid derivatives (2–10, 2b, 3a, 3b, 6a–16a, 7b, 9b, 10b, 13, 15–26, 15b, 18a, 23a, 27a) were prepared by C-11 and -15 esterification of 1. Antiproliferative effects of the natural parent compound (1) and all synthesized kobusine derivatives against human cancer cell lines, including a triple-negative breast cancer (TNBC) cell line as well as a P-glycoprotein overexpressing multidrug-resistant subline, were assessed. The structure-based design strategy resulted in the lead derivative 11,15-dibenzoylkobusine (3; average IC₅₀ 7.3 μM). Several newly synthesized kobusine derivatives (particularly, 5–8, 10, 13, 15–26) exhibited substantial suppressive effects against all tested human cancer cell lines. In contrast, kobusine (1), 11,15-O-diacetylkobusine (2), 11-acylkobusine derivatives (3a, 6a, 9a, 11a, 12a, 15a, 27a), and 15-acylkobusine derivatives (2b, 3b, 7b, 9b, 10b, 15b) showed no effect. The most active kobusine derivatives primarily had two specific substitution patterns, C-11,15 and C-11. Notably, 11,15-diacylkobusine derivatives (3, 6–10, 13, 15, 16, 18, 23) were more potent compared with 11- and 15-acylkobusine derivatives (3a, 3b, 6a–10a, 7b, 9b, 10b, 13a, 15a, 15b, 16a, 18a, 23a). Derivatives 13 and 25 induced MDA-MB-231 cells to the sub-G1 phase within 12 h. 11,15-Diacylation of kobusine (1) appears to be crucial for inducing antiproliferative activity in this alkaloid class and could introduce a new avenue to overcome TNBC using natural product derivatives.

INTRODUCTION

Chemotherapy refers primarily to the usage of cytotoxic small molecules for cancer treatment, and natural products are major sources of currently available chemotherapeutics. Based on a review of New Chemical Entities (NCE) from 1981 to 2019, nearly 75% of antitumor agents are not purely synthetic compounds, with 47% either being natural products including their derivatives or mimicking natural products.¹ A great variety of chemically and biologically active anticancer agents are used in cancer chemotherapy, and classical plant alkaloids such as vincristine and paclitaxel are still commonly used in clinical practice.^{2–10} While studies on the phytochemistry and synthetic and medicinal chemistry of diterpenoid alkaloids have led to the discovery of remarkable pharmacological activities and structural complexity, little facts at the antiproliferative properties have been reported.

A large number of diterpenoid alkaloids isolated from various species of *Aconitum* and *Delphinium* (*Ranunculaceae*) have been identified as the main bioactive constituents related to both toxicity and medical uses.¹¹ These diterpenoid alkaloids are categorized in line with their chemical structure as C₁₉-diterpenoid alkaloids, which have a lycotoxine or an aconitine skeleton, and C₂₀-diterpenoid alkaloids, which have a veatchine or an atisine skeleton.¹² The former group contains aconitine, mesaconitine, hyaconitine, and jesaconitine, which are extraordinarily toxic, while compounds in the latter group,

Received: April 15, 2022

Accepted: July 25, 2022

Published: August 4, 2022



together with lucidusculine, kobusine (1), pseudokobusine, and atisine, are much less toxic.¹¹ The pharmacological properties of the C₁₉-diterpenoid alkaloids have been studied expansively and reviewed.¹³ However, the pharmacological characteristics of the C₂₀-diterpenoid alkaloids and their derivatives have been less investigated.

Our earlier study confirmed the effects of several semi-synthetic and natural diterpenoid alkaloids on growth of the A172 human malignant glioma cell line.¹⁴ Effects of various types of novel diterpenoid alkaloid derivatives on antiproliferation and radiosensitization were also studied.¹⁵ Two novel hetisine-type C₂₀-diterpenoid derivatives exhibited noteworthy suppressive effects against the Raji non-Hodgkin's lymphoma cell line.¹⁶ Moreover, the effects of several novel hetisine-type C₂₀-diterpenoid alkaloid derivatives on the growth of the A549 human lung cancer cells were examined, and subsequent structure–activity relationships (SAR) for the antiproliferative activities against A549 cells were reported.¹⁷ In previous pharmacological studies, several diterpenoid alkaloids and their derivatives displayed antiproliferative activity against several human cancer cell lines, including A549 (lung carcinoma), DU145 (prostate carcinoma), KB (cervical carcinoma HeLa derivative), and its MDR subline KB-VIN (P-gp over-expressing vincristine-resistant KB subline).^{18,19} As recently reported, we evaluated lycocotinine-type C₁₉-diterpenoid alkaloids, delcosine, 14-acetyldelcosine, and 14-acetylbrowniine, and synthesized derivatives for antiproliferative effects against five human cancer cell line panels {A549, MDA-MB-231 [triple-negative breast cancer (TNBC), hormone receptor-negative and HER2-negative], MCF-7 (estrogen receptor-positive, HER2-negative breast cancer), KB, and KB-VIN}.²⁰ Among such diterpenoid alkaloids, lycocotinine-type C₁₉-diterpenoid and C₂₀-diterpenoid alkaloid derivatives exhibited significant antiproliferative activity and, thus, provided promising novel leads for further development as antineoplastic agents. Less data are available regarding the antiproliferative properties of natural hetisine-type C₂₀-diterpenoid alkaloids as well as their derivatives. However, 11,15-dibenzoylkobusine (3) exhibited significant potency against A549, KB, and KB-VIN cell lines (average IC₅₀ 7.3 μM), although the natural parent alkaloid kobusine (1), a hetisine-type C₂₀-diterpenoid alkaloid, and 11,15-diacetylkobusine (2) were inactive (IC₅₀ > 20 μM) against the same three cell lines.¹⁹ Therefore, in this current study, prior and newly synthesized kobusine derivatives were evaluated for antiproliferative activity against five human cancer cell line panels (A549, MDA-MB-231, MCF-7, KB, and KB-VIN).

RESULTS AND DISCUSSION

Kobusine (1), a hetisine-type C₂₀-diterpenoid alkaloid, was purified from *Aconitum yesoense* var. *macroyesoense* (NAKAI) TAMURA (*Ranunculaceae*) by a previously described procedure.^{21,22} Kobusine (1) was reacted with various acyl chlorides in pyridine (Figure 1) to give C-11-, C-15-, or C-11,15-substituted acyl derivatives (4–10, 13, 15–26, 3a, 3b, 6a–16a, 7b, 9b, 10b, 15b, 18a, 23a, 27a) (Figure 2). The synthesized derivatives (4, 5, 7–9, 7a–9a, 7b, 9b, 13, 13a, 16–25, 16a, 18a, 23a) were evaluated for antiproliferative activity against our five human cancer cell line panels. Paclitaxel was used as an experimental control (data shown in Table 1). In this study, previously synthesized 18 derivatives (2, 2b, 3, 3a, 3b, 6, 6a, 10, 10a–12a, 10b, 14a, 15, 15a, 15b,

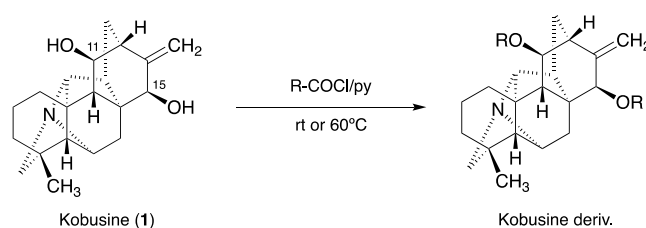


Figure 1. Synthesis of kobusine derivatives.

26, 27a) were evaluated for antiproliferative activity against human cancer cell lines [A549, DU145, KB, and KB-VIN].¹⁹

With three exceptions [11-acyl derivatives 11a, 12a, and 27a, containing a 2-trifluoromethylbenzoyl, 3-trifluoromethylbenzoyl, or nicotinoyl group, respectively, were inactive (IC₅₀ > 20 μM)], acylation of the C-11 and/or C-15 hydroxy group of kobusine (1) led to various degrees of antiproliferative activity. Among the derivatives esterified at both C-11 and -15, derivatives 5 [11,15-di-(3-methoxybenzoyl)kobusine], 6 [11,15-dianisoylkobusine], 7 [11,15-di-(3,4,5-trimethoxybenzoyl)kobusine], 8 [11,15-di-(4-ethoxybenzoyl)kobusine], 10 [11,15-di-*p*-nitrobenzoylkobusine], 13 [11,15-di-(4-trifluoromethylbenzoyl)kobusine], 15 [11,15-di-(4-fluorobenzoyl)kobusine], 16 [11,15-di-(4-fluoro-3-methylbenzoyl)kobusine], 17 [11,15-di-(3-chloro-4-fluorobenzoyl)kobusine], 18 [11,15-di-(2,4,5-trifluoro-3-methoxybenzoyl)kobusine], 19 [11,15-di-(1,2,3,4,5,6-pentafluorobenzoyl)kobusine], 20 [11,15-di-(2-chlorobenzoyl)kobusine], 21 [11,15-di-(3-chlorobenzoyl)kobusine], 22 [11,15-di-(4-chlorobenzoyl)kobusine], 23 [11,15-di-(3,5-dichlorobenzoyl)kobusine], 24 [11,15-di-(4-chloro-3-nitrobenzoyl)kobusine], 25 [11,15-di-(4-dichloromethylbenzoyl)kobusine], and 26 [11,15-di-(3-trifluoromethylcinnamoyl)kobusine] exhibited significant potency against three to five human cancer cell lines (average IC₅₀ 4.2–6.8). Derivatives 4 [11,15-di-(2-methoxybenzoyl)kobusine] and 9 [11,15-di-(3-nitrobenzoyl)kobusine] showed moderate potency against all five human cancer cell lines (average IC₅₀ 15.7 and 18.8 μM, respectively). Although derivative 4 displayed good antiproliferative activity against MCF-7 and KB cells (IC₅₀ 13.4 and 13.0 μM, respectively), it was much less active against A549, MDA-MB-231, and KB-VIN cells.

Among the C-11 esterified derivatives, derivatives 8a [11-(4-ethoxybenzoyl)kobusine], 10a [11-*p*-nitrobenzoylkobusine], 13a [11-(4-trifluoromethylbenzoyl)kobusine], and 14a [11-(4-trifluoromethoxybenzoyl)kobusine] exhibited moderate potency against three to five tested cell lines (average IC₅₀ 12.4, 17.1, 19.0, and 12.2 μM, respectively). Derivative 8a showed significant antiproliferative activity against A549, KB, and KB-VIN cells (IC₅₀ 7.8, 8.9, and 11.2 μM, respectively) but was less active against MDA-MB-231 and MCF-7 (IC₅₀ 15.9 and 18.0 μM, respectively). Derivatives 7a [11-(3,4,5-trimethoxybenzoyl)kobusine], 16a [11-(4-fluoro-3-methylbenzoyl)kobusine], and 18a [11-(2,4,5-trifluoro-3-methoxybenzoyl)kobusine] exhibited only weak potency against all five human cancer cell lines (average IC₅₀ 23.3, 30.4, and 27.7 μM, respectively). Derivatives 3a, 6a, 9a, 11a, 12a, 15a, and 27a were inactive against all tested human cancer cell lines. All five C-15 esterified derivatives, 3b, 7b, 9b, 10b, and 15b, were also inactive against all tested human cancer cell lines.

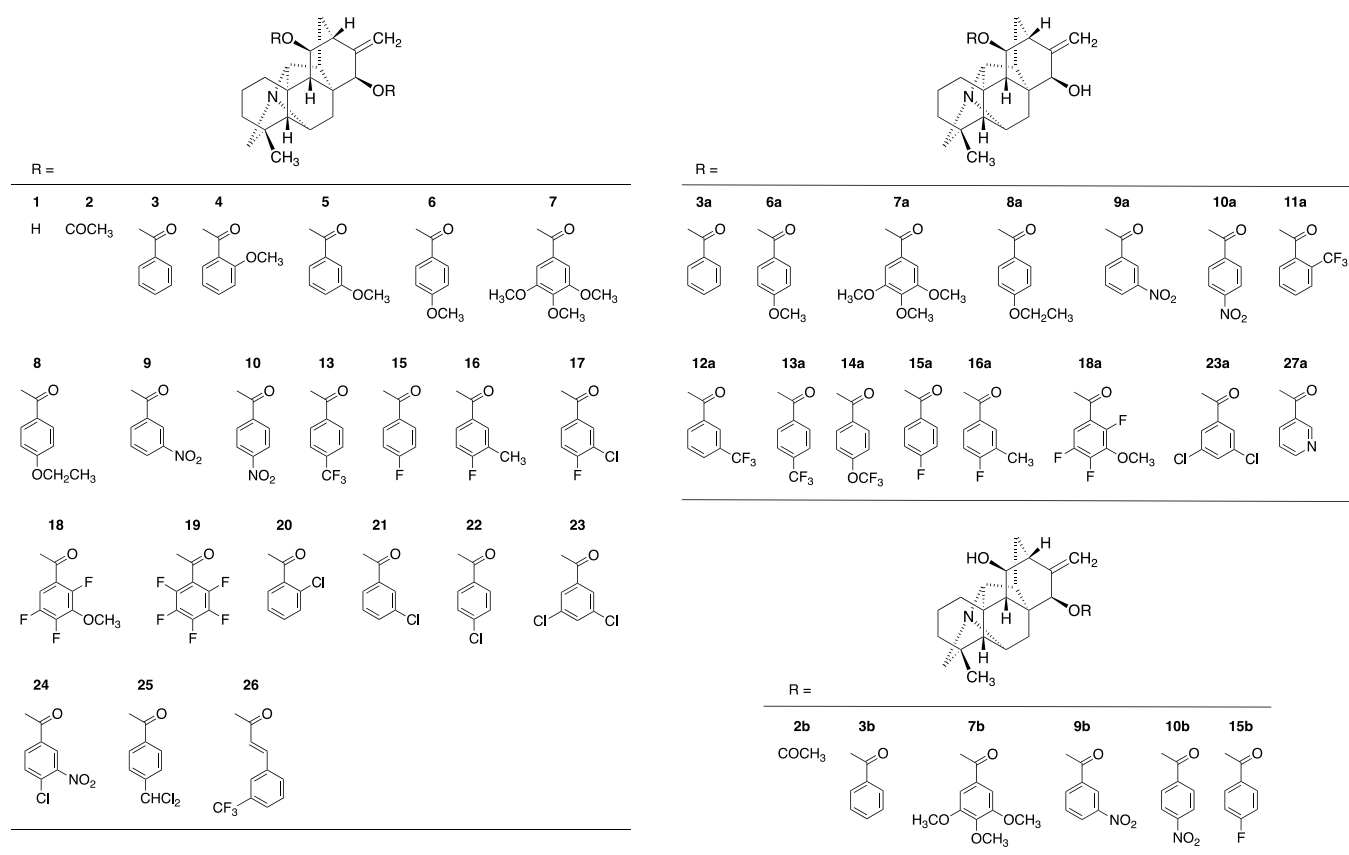


Figure 2. Chemical structures of derivatives 1–27a.

Particularly, C-11,15 diacylated kobusine derivatives (3, 6–10, 13–16, 18) showed significantly better potency compared with the corresponding C-11 or -15 monoacylated kobusine derivatives (3a, 3b, 6a–10a, 7b, 9b, 10b, 13a–16a, 18a). Thus, C-11,15 diesterification was crucial for enhanced antiproliferative activity of kobusine (1) derivatives.

Prominent observations from the data in Table 1 were the reliable identities of the most active derivatives. Kobusine derivatives 5–8, 10, 13, and 16–26 displayed the highest potency against all tested cancer cell lines with IC_{50} values ranging from 2.8 to 6.9 μM . A similar range of potency was found with derivatives 3 and 15 against KB cells (6.0 and 5.2 μM , respectively). The potencies of 3, 8a, and 15 (IC_{50} 5.2–11.2 μM) generally graded somewhat below those of the most potent derivatives, except against MDA-MB-231 and MCF-7 cell lines, where they were even less active. Derivative 14a showed moderate activity against KB and KB-VIN (11.7 and 10.9 μM , respectively).

The identity of the substituent(s) on the acyl group affected the cytotoxic potency. Notably, among the C-11,15 disubstituent derivatives, derivatives 5–8, 10, 13, and 16–26 with variously substituted benzoyl or cinnamoyl esters showed significant potency against all tested human cancer cell lines. Among derivatives with small alkoxy groups on the benzoate esters, 5 (3-methoxy), 6 (4-methoxy), 7 (3,4,5-trimethoxy), and 8 (4-ethoxy) were more potent than 4 (2-methoxy). Derivative 5 (3-methoxybenzoyl) was more potent than 6 (4-methoxybenzoyl), and derivative 7 with 3,4,5-trimethoxy substitution on the benzoate ester was more potent than 5 with the 3-methoxy group. Also, derivative 10 with a 4-nitro moiety was more potent than 9 with the 3-nitro group.

Further, the fluorinated derivatives 16 (4-fluoro-3-methyl), 17 (3-chloro-4-fluoro), 18 (2,4,5-trifluoro-3-methoxy), and 19 (2,3,4,5,6-pentafluoro) were more potent than 15 with only a single 4-fluoro substituent. Similarly, derivatives 13 (4-trifluoromethylbenzoate) and 26 (3-trifluoromethylcinnamate) showed increased antiproliferative activity against the three to five cancer cell lines compared with 4-fluorinated derivative 15. The fluorinated derivatives (13, 16–19, and 26: average IC_{50} 4.9) were more potent than derivatives with small alkoxy groups (4–8: average IC_{50} 7.1) and nitro groups (9, 10, and 24: average IC_{50} 9.9) on the benzoate esters. Moreover, the 3-, 4-, or 3,5-chlorinated derivatives 21–24 as well as 25, which has 4-dichloromethyl substitution on the benzoate ester, were more potent than 20 with only a single 2-chloro substituent. Derivatives 21 (3-chlorobenzoyl) and 23 (3,5-dichlorobenzoyl) were equipotent and more potent than 22 (4-chlorobenzoyl) and 24 (4-chloro-3-nitrobenzoate), which were also equipotent.

Additionally, among 17 derivatives (5–8, 10, 13, and 16–26), 13 derivatives (5, 7, 8, 13, 16–19, and 21–25) exhibited significant potency against MDA-MB-231 cell lines with IC_{50} values ranging from 2.8 to 5.0 μM . Particularly, derivative 22 (4-chlorobenzoyl, IC_{50} 2.8 μM) exhibited the highest potency against this cell line. Meanwhile, the IC_{50} values for the same 13 derivatives (5, 7, 8, 13, 16–19, and 21–25) ranged from 4.2 to 5.3 μM against the MCF-7 cell line. A similar range of potency (IC_{50} 4.4–5.5 μM) was found with 15 derivatives (5, 7, 8, 13, and 16–26) against the A549 cell line. Furthermore, derivatives 5–8, 10, 13, and 15–26 were potent against the KB cell line with IC_{50} values ranging from 4.1 to 5.3 μM . Moreover, derivatives 5–8, 10, 13, and 16–26 exhibited

Table 1. Antiproliferative Activity of Kobusine (1) and Derivatives 2–27a

alkaloid	cell line/IC ₅₀ (μM) ^a				
	AS49	MDA-MB-231	MCF-7	KB	KB-VIN
1 ^c	>20			>20	>20
2 ^c	>20			>20	>20
2b ^c	>20			>20	>20
3 ^c	8.4			6.0	7.5
3a ^c	>20			>20	>20
3b ^c	>20			>20	>20
4	17.0	19.0	13.4	13.0	16.1
5	4.5	4.5	4.7	4.7	4.8
6 ^c	6.7			5.3	5.2
6a ^c	>20			>20	>20
7	4.4	4.7	4.2	4.2	4.6
7a	19.5	21.2	26.9	19.9	28.9
7b	>40	>40	>40	>40	>40
8	4.5	4.6	5.2	4.6	5.0
8a	7.8	15.9	18.0	8.9	11.2
9	19.5	19.9	18.3	17.4	19.1
9a	>40	>40	>40	>40	>40
9b	>40	>40	>40	>40	>40
10 ^c	6.9			5.3	5.5
10a ^c	19.5			13.9	17.9
10b ^c	>20			>20	>20
11a ^c	>20			>20	>20
12a ^c	>20			>20	>20
13	4.8	4.5	4.7	4.6	4.8
13a	18.1	19.3	19.6	18.1	20.1
14a ^c	14.1			11.7	10.9
15c	8.1			5.2	7.1
15a ^c	>20			>20	>20
15b ^c	>20			>20	>20
16	4.6	4.8	4.9	4.5	4.7
16a	30.0	32.1	29.5	27.1	33.2
17	4.5	4.6	4.6	4.4	4.6
18	4.5	5.0	4.6	4.7	4.6
18a	27.9	26.8	23.8	28.7	31.1
19	4.5	4.4	4.7	4.5	5.2
20	5.3	6.4	6.3	5.1	5.6
21	4.4	4.7	4.7	4.7	4.6
22	4.5	2.8	5.3	5.1	5.7
23	4.4	4.5	4.5	4.6	4.6
23a	20.4	21.0	18.6	21.5	21.0
24	5.2	4.4	5.3	4.8	5.7
25	4.4	4.2	4.5	4.5	4.6
26 ^c	5.5			4.1	3.1
27a ^c	>20			>20	>20
paclitaxel ^b	0.0052	0.0067	0.0073	0.0050	1.3

^aAntiproliferative activity as IC₅₀ values for each cell line, the concentration of the derivative that caused 50% reduction in growth relative to untreated cells as determined by the SRB assay. ^bPaclitaxel was used as an experimental control. ^cSee ref 19.

significant potency against the KB-VIN cell line with IC₅₀ values ranging from 3.1 to 5.7 μM. Particularly, derivative **26** (3-trifluoromethylcinnamate, IC₅₀ 3.1 μM) exhibited the highest potency against the KB-VIN cell line. Many derivatives displayed comparable potency against the KB and KB-VIN cell lines, in contrast to paclitaxel.

The 11-monoacylated derivatives with moderate potency against the three to five tested cancer cell lines contained 4-ethoxy- (**8a**) and 4-trifluoromethoxy- (**14a**) benzoyl esters. Furthermore, with some exceptions against certain cell lines, derivatives with unsubstituted (**3a**), methoxy (**6a**), trimethoxy

(**7a**), nitro (**9a**, **10a**), trifluoromethyl (**11a**–**13a**), fluoro (**15a**), 4-fluoro-3-methyl (**16a**), 2,4,5-trifluoro-3-methoxy (**18a**), and 3,5-dichloro (**23a**) substituted benzoate esters or nicotinoyl (**27a**) ester were less active or inactive. In contrast, the 15-monoacylated derivatives **3b**, **7b**, **9b**, **10b**, and **15b** were inactive against all three to five tested cancer cell lines.

Intriguingly, the potent derivatives were generally effective against the P-gp-overexpressing MDR subline KB-VIN, while alkaloids such as paclitaxel and vincristine are less effective due to excretion from the MDR cells by P-gp. These results indicate that these derivatives are not substrates for P-gp.

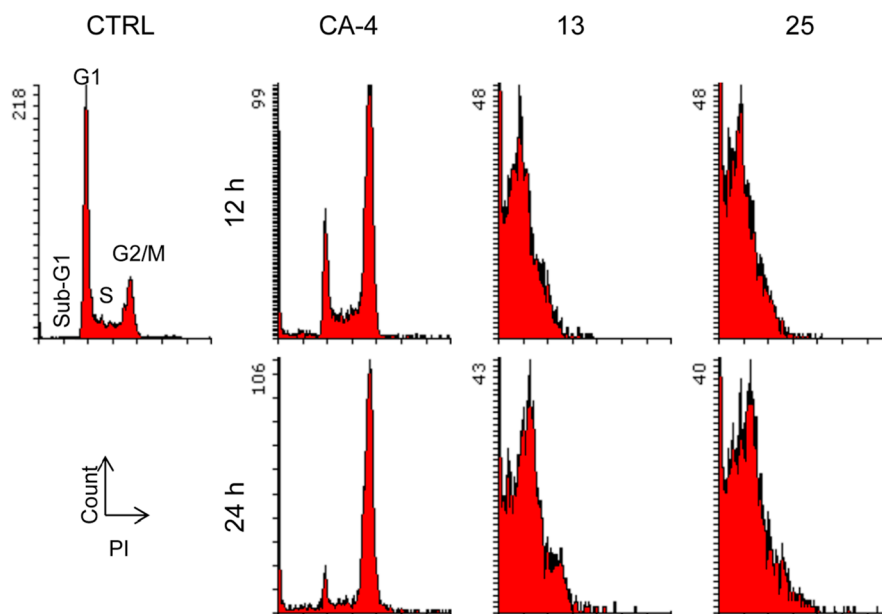


Figure 3. Effects of derivatives **13** and **25** on the cell cycle. MDA-MB-231 (TNBC) cells were treated for 12 or 24 h with derivatives at a 3-fold ($3 \times IC_{50}$) concentration of their IC_{50} . DMSO (CTRL) or $0.2 \mu M$ ($3 \times IC_{50}$) combretastatin A-4 (CA-4) was used as a vehicle control or a tubulin polymerization inhibitor arresting cells in G2/M, respectively. Cell cycle distributions of treated cells were assessed by flow cytometry (LSRII) after staining with PI in the presence of RNase.

To address the mechanism of action (MOA) of the kobusine (**1**) derivatives, we further examined the effects of derivatives on cell cycle progression. The TNBC cell line MDA-MB-231 was treated for 12 or 24 h with derivatives at threefold ($3 \times IC_{50}$) concentrations of their IC_{50} . DMSO (CTRL) or $0.2 \mu M$ ($3 \times IC_{50}$) combretastatin A-4 (CA-4) was used as a vehicle control or a tubulin polymerization inhibitor arresting cells at G2/M, respectively. Cell cycle distributions of treated cells were analyzed by flow cytometry (LSRII) after staining with propidium iodide (PI) in the presence of RNase. Time-course studies were carried out at 12 and 24 h using derivatives at $3 \times IC_{50}$ (Figure 3). With all derivatives tested, sub-G1 cells heavily accumulated after 12 h treatment at $3 \times IC_{50}$, while normal cell cycle progression was disrupted after 12 h treatment with **13** and **25** with decreasing numbers of cells in S and G2/M phases, resulting in accumulation of sub-G1. These results proved that derivatives **13** and **25** act through a similar MOA to induce sub-G1 accumulation within 12 h. In general, sub-G1 cells undergo apoptosis, unlike cytotoxicity. These observations suggested that derivatives **13** and **25** likely induced apoptosis within 12 h, but a detailed MOA analysis should be required to determine whether sub-G1 accumulation is due to apoptosis induction.

CONCLUSIONS

C-11 and -15 acylations of kobusine (**1**), a hetisine-type C_{20} -diterpenoid alkaloid, were carried out to provide 43 novel derivatives (**2–10**, **2b**, **3a**, **3b**, **6a–16a**, **7b**, **9b**, **10b**, **13**, **15–26**, **15b**, **18a**, **23a**, **27a**). The natural alkaloid **1** and all synthesized derivatives (**2–10**, **2b**, **3a**, **3b**, **6a–16a**, **7b**, **9b**, **10b**, **13**, **15–26**, **15b**, **18a**, **23a**, **27a**) were evaluated for antiproliferative activity against A549, MDA-MB-231, MCF-7, KB, and KB-VIN cancer cell lines. Several newly synthesized kobusine derivatives (particularly, **3**, **5–8**, **10**, **13**, **15–26**) showed significant suppressive effects against these cell lines. In contrast, kobusine (**1**), 11,15-O-diacetylkobusine (**2**), 11-

acylkobusine derivatives (**3a**, **6a**, **9a**, **11a**, **12a**, **15a**, **27a**) and 15-acylkobusine derivatives (**2b**, **3b**, **7b**, **9b**, **10b**, **15b**) showed no effect. Among the active acyl derivatives, most 11,15-diacetylkobusine derivatives (**3**, **6–10**, **13**, **15**, **16**, **18**, **23**) showed more potency compared with 11- and 15-acylkobusine derivatives (**3a**, **3b**, **6a–10a**, **7b**, **9b**, **10b**, **13a**, **15a**, **15b**, **16a**, **18a**, **23a**). Derivatives **13** and **25** induced accumulation of sub-G1 cells within 12 h. 11,15-Diacylation of **1** as a lead appears to be critical for producing antiproliferative activity in this hetisine-type C_{20} -diterpenoid alkaloid class. Continual studies are merited to demonstrate the molecular MOA of sub-G1 accumulation by treatment with derivatives.

EXPERIMENTAL SECTION

Chemistry. IR spectra were recorded using a SHIMADZU model IRAffinity-1S (Shimadzu, Kyoto, Japan). NMR spectra were recorded in $CDCl_3$ on a JEOL model ECZ400 spectrometer (JEOL, Tokyo, Japan) with TMS as an internal standard. Mass spectrometry and high-resolution mass spectrometry were performed on a JEOL model JMS-700 mass spectrometer (JEOL, Tokyo, Japan).

Alkaloids. Kobusine (**1**) was extracted from *A. yesoense* var. *macroyesoense*, followed by purification and identification by methods described previously.^{21,22} A total of 18 acyl derivatives, 11,15-O-diacetylkobusine (**2**),²³ 15-O-acetylkobusine (**2b**),²³ 11,15-dibenzoylkobusine (**3**),²³ 11-benzoylkobusine (**3a**),²³ 15-benzoylkobusine (**3b**),²³ 11,15-dianisoylkobusine (**6**),²⁴ 11-anisoylkobusine (**6a**),²⁴ 11,15-di-*p*-nitrobenzoylkobusine (**10**),¹⁷ 11-*p*-nitrobenzoylkobusine (**10a**),¹⁷ 15-*p*-nitrobenzoylkobusine (**10b**),¹⁷ 11-(2-trifluoromethylbenzoyl)kobusine (**11a**),¹⁹ 11-(3-trifluoromethylbenzoyl)kobusine (**12a**),¹⁴ 11-(4-trifluoromethoxybenzoyl)kobusine (**14a**),¹⁹ 11,15-di-(4-fluorobenzoyl)kobusine (**15**),¹⁹ 11-(4-fluorobenzoyl)kobusine (**15a**),¹⁹ 15-(4-fluorobenzoyl)kobusine (**15b**),¹⁹ 11,15-di-(3-trifluoromethylcinnamoyl)-

kobusine (26),¹⁹ and 11-(nicotinoyl)kobusine (27a),²⁴ were prepared by methods described previously.

General Procedure for the Synthesis of Kobusine Analogues. Kobusine (1) and an acyl chloride dissolved in pyridine were stirred at 60 °C (derivatives 13 and 18) or room temperature under Ar. The reaction solution was quenched with water, and ammonia water was added to pH 10. The reaction solution was extracted with CHCl₃ (three times). The combined organic layers were washed with saturated aq. NaHCO₃ and brine and dried over anhydrous MgSO₄. Then, the solvent was removed in vacuo. The crude products were purified by silica gel column chromatography eluting with *n*-hexane–CHCl₃ saturated with 28% aq. NH₃.

11,15-Di-(2-methoxybenzoyl)kobusine (4). 39% yield; colorless amorphous solid; HR–FABMS *m/z*: 582.2849 [M + H]⁺ calcd for C₃₆H₄₀NO₆, 582.2856; IR (ATR) ν_{\max} cm⁻¹: 2928, 2859, 1721, 1601, 1581, 1234, 1130, 1022, 953; ¹H NMR (CDCl₃): δ 0.99 (3H, s, 18-CH₃), 3.78 and 3.84 (each 3H, s, OCH₃), 5.10 and 5.35 (each 1H, s, C=CH₂), 5.39 (1H, d, *J* = 4.5 Hz, 11-H), 5.77 (1H, s, 15-H), 6.36 and 6.71 (each 1H, t, *J* = 8.2 Hz, Ar–H), 6.87 (2H, d, *J* = 8.2 Hz, Ar–H), 7.32 and 7.40 (each 1H, t, *J* = 8.2 Hz, Ar–H), 7.73 and 7.77 (each 1H, d, *J* = 8.2 Hz, Ar–H); FABMS *m/z*: 582 [M + H]⁺.

11,15-Di-(3-methoxybenzoyl)kobusine (5). 76% yield; colorless amorphous solid; HR–FABMS *m/z*: 582.2867 [M + H]⁺ calcd for C₃₆H₄₀NO₆, 582.2856; IR (ATR) ν_{\max} cm⁻¹: 2924, 2855, 1740, 1721, 1585, 1219, 1103, 1038, 957; ¹H NMR (CDCl₃): δ 0.95 (3H, s, 18-CH₃), 3.59 and 3.65 (each 3H, s, OCH₃), 5.15 and 5.36 (each 1H, s, C=CH₂), 5.46 (1H, d, *J* = 4.5 Hz, 11-H), 5.79 (1H, s, 15-H), 7.00 and 7.01 (each 1H, t, *J* = 8.2 Hz, Ar–H), 7.08 and 7.10 (each 1H, dd, *J* = 8.2, 2.7 Hz, Ar–H), 7.48 and 7.50 (each 1H, s, Ar–H), 7.51 and 7.57 (each 1H, d, *J* = 8.2 Hz, Ar–H); FABMS *m/z*: 582 [M + H]⁺.

11,15-Di-(3,4,5-trimethoxybenzoyl)kobusine (7). 15% yield; colorless amorphous solid; HR–FABMS *m/z*: 702.3277 [M + H]⁺ calcd for C₄₀H₄₈NO₁₀, 702.3278; IR (ATR) ν_{\max} cm⁻¹: 2940, 2851, 1740, 1589, 1219, 1126, 995; ¹H NMR (CDCl₃): δ 0.96 (3H, s, 18-CH₃), 3.51 and 3.56 (each 6H, s, Ar-OCH₃), 3.81 and 3.82 (each 3H, s, Ar-OCH₃), 5.21 and 5.42 (each 1H, s, C=CH₂), 5.47 (1H, d, *J* = 5.0 Hz, 11-H), 5.81 (1H, s, 15-H), 7.16 and 7.26 (each 2H, s, Ar–H); FABMS *m/z*: 702 [M + H]⁺.

11-(3,4,5-Trimethoxybenzoyl)kobusine (7a). 35% yield; colorless amorphous solid; HR–FABMS *m/z*: 508.2692 [M + H]⁺ calcd for C₃₀H₃₈NO₆, 508.2699; IR (ATR) ν_{\max} cm⁻¹: 3449, 2940, 2866, 1713, 1589, 1219, 1123, 1034, 1003, 961; ¹H NMR (CDCl₃): δ 0.98 (3H, s, 18-CH₃), 3.87 (6H, s, Ar-OCH₃), 3.90 (3H, s, Ar-OCH₃), 4.01 (1H, d, *J* = 8.2 Hz, 15-H), 5.12 and 5.29 (each 1H, s, C=CH₂), 5.38 (1H, d, *J* = 5.0 Hz, 11-H), 7.24 (2H, s, Ar–H); FABMS *m/z*: 508 [M + H]⁺.

15-(3,4,5-Trimethoxybenzoyl)kobusine (7b). 12% yield; colorless amorphous solid; HR–FABMS *m/z*: 508.2726 [M + H]⁺ calcd for C₃₀H₃₈NO₆, 508.2699; IR (ATR) ν_{\max} cm⁻¹: 3449, 2924, 2851, 1736, 1589, 1227, 1130, 1038, 988; ¹H NMR (CDCl₃): δ 0.97 (3H, s, 18-CH₃), 3.91 (6H, s, Ar-OCH₃), 3.92 (3H, s, Ar-OCH₃), 4.09 (1H, bs, 11-H), 5.24 and 5.38 (each 1H, s, C=CH₂), 5.71 (1H, s, 15-H), 7.30 (2H, s, Ar–H); FABMS *m/z*: 508 [M + H]⁺.

11,15-Di-(4-ethoxybenzoyl)kobusine (8). 15% yield; colorless amorphous solid; HR–FABMS *m/z*: 610.3156 [M + H]⁺ calcd for C₃₈H₄₄NO₆, 610.3169; IR (ATR) ν_{\max} cm⁻¹: 2928, 2866, 1736, 1605, 1250, 1169, 1042, 957; ¹H NMR (CDCl₃):

δ 0.98 (3H, s, 18-CH₃), 1.38 and 1.41 (each 3H, t, *J* = 7.2 Hz, OCH₂CH₃), 3.98 (4H, q, *J* = 7.2 Hz, OCH₂CH₃), 5.12 and 5.35 (each 1H, s, C=CH₂), 5.40 (1H, d, *J* = 5.0 Hz, 11-H), 5.74 (1H, s, 15-H), 6.65 (4H, d, *J* = 8.6 Hz, Ar–H), 7.84 and 7.88 (each 2H, d, *J* = 8.6 Hz, Ar–H); FABMS *m/z*: 610 [M + H]⁺.

11-(4-Ethoxybenzoyl)kobusine (8a). 30% yield; colorless amorphous solid; HR–FABMS *m/z*: 462.2656 [M + H]⁺ calcd for C₂₉H₃₆NO₄, 462.2644; IR (ATR) ν_{\max} cm⁻¹: 3456, 2943, 2866, 1740, 1605, 1213, 1111, 1038; ¹H NMR (CDCl₃): δ 0.99 (3H, s, 18-CH₃), 1.44 (3H, t, *J* = 7.2 Hz, OCH₂CH₃), 4.00 (1H, s, 15-H), 4.08 (2H, q, *J* = 7.2 Hz, OCH₂CH₃), 5.09 and 5.27 (each 1H, s, C=CH₂), 5.36 (1H, d, *J* = 5.0 Hz, 11-H), 6.89 and 7.89 (each 2H, d, *J* = 8.6 Hz, Ar–H); FABMS *m/z*: 462 [M + H]⁺.

11,15-Di-(3-nitrobenzoyl)kobusine (9). 47% yield; colorless amorphous solid; HR–FABMS *m/z*: 612.2354 [M + H]⁺ calcd for C₃₄H₃₄N₃O₈, 612.2346; IR (ATR) ν_{\max} cm⁻¹: 2924, 2851, 1717, 1616, 1531, 1354, 1258, 1134, 1072, 957; ¹H NMR (CDCl₃): δ 0.98 (3H, s, 18-CH₃), 5.20 and 5.43 (each 1H, s, C=CH₂), 5.55 (1H, d, *J* = 4.5 Hz, 11-H), 5.86 (1H, s, 15-H), 7.44 and 7.50 (each 1H, t, *J* = 8.2 Hz, Ar–H), 8.28 (4H, m, Ar–H), 8.63 and 8.70 (each 1H, t, *J* = 1.8 Hz, Ar–H); FABMS *m/z*: 612 [M + H]⁺.

11-(3-Nitrobenzoyl)kobusine (9a). 11% yield; colorless amorphous solid; HR–FABMS *m/z*: 463.2261 [M + H]⁺ calcd for C₂₇H₃₁N₂O₅, 463.2233; IR (ATR) ν_{\max} cm⁻¹: 3429, 2924, 2855, 1724, 1616, 1528, 1346, 1250, 1134, 1072, 957; ¹H NMR (CDCl₃): δ 0.99 (3H, s, 18-CH₃), 4.06 (1H, s, 15-H), 5.10 and 5.27 (each 1H, s, C=CH₂), 5.42 (1H, d, *J* = 4.1 Hz, 11-H), 7.64 (1H, t, *J* = 8.2 Hz, Ar–H), 8.27 and 8.41 (each 1H, d, *J* = 8.2 Hz, Ar–H), 8.82 (1H, s, Ar–H); FABMS *m/z*: 463 [M + H]⁺.

15-(3-Nitrobenzoyl)kobusine (9b). 7% yield; colorless amorphous solid; HR–FABMS *m/z*: 463.2261 [M + H]⁺ calcd for C₂₇H₃₁N₂O₅, 463.2233; IR (ATR) ν_{\max} cm⁻¹: 3456, 2924, 2855, 1724, 1616, 1531, 1350, 1258, 1134, 1072, 961; ¹H NMR (CDCl₃): δ 0.96 (3H, s, 18-CH₃), 4.14 (1H, bs, 11-H), 5.26 and 5.40 (each 1H, s, C=CH₂), 5.76 (1H, s, 15-H), 7.67 (1H, t, *J* = 8.2 Hz, Ar–H), 8.34 and 8.44 (each 1H, d, *J* = 8.2 Hz, Ar–H), 8.87 (1H, s, Ar–H); FABMS *m/z*: 463 [M + H]⁺.

11,15-Di-(4-trifluoromethylbenzoyl)kobusine (13). 86% yield; colorless amorphous solid; HR–FABMS *m/z*: 658.2381 [M + H]⁺ calcd for C₃₆H₃₄F₆NO₄, 658.2392; IR (ATR) ν_{\max} cm⁻¹: 2932, 2870, 1717, 1585, 1258, 1119, 1065, 953; ¹H NMR (CDCl₃): δ 0.97 (3H, s, 18-CH₃), 5.17 and 5.39 (each 1H, s, C=CH₂), 5.49 (1H, d, *J* = 4.5 Hz, 11-H), 5.80 (1H, s, 15-H), 7.42, 7.44, 7.98 and 8.02 (each 2H, d, *J* = 8.6 Hz, Ar–H); FABMS *m/z*: 658 [M + H]⁺.

11-(4-Trifluoromethylbenzoyl)kobusine (13a). 8% yield; colorless amorphous solid; HR–FABMS *m/z*: 486.2256 [M + H]⁺ calcd for C₂₈H₃₁F₃NO₃, 486.2256; IR (ATR) ν_{\max} cm⁻¹: 3333, 2920, 2851, 1717, 1601, 1582, 1277, 1123, 1065; ¹H NMR (CDCl₃): δ 1.08 (3H, s, 18-CH₃), 4.10 (1H, s, 15-H), 5.13 and 5.28 (each 1H, s, C=CH₂), 5.35 (1H, d, *J* = 4.5 Hz, 11-H), 7.69 and 8.05 (each 2H, d, *J* = 8.1 Hz, Ar–H); FABMS *m/z*: 486 [M + H]⁺.

11,15-Di-(4-fluoro-3-methylbenzoyl)kobusine (16). 45% yield; colorless amorphous solid; HR–FABMS *m/z*: 586.2764 [M + H]⁺ calcd for C₃₆H₃₈F₂NO₄, 586.2769; IR (ATR) ν_{\max} cm⁻¹: 2928, 2866, 1709, 1593, 1231, 1115, 1022, 957; ¹H NMR (CDCl₃): δ 0.96 (3H, s, 18-CH₃), 2.00 and 2.02

(each 3H, d, $J = 1.8$ Hz, Ar-CH₃), 5.14 and 5.37 (each 1H, s, C=CH₂), 5.46 (1H, d, $J = 4.5$ Hz, 11-H), 5.77 (1H, s, 15-H), 6.83 and 6.86 (each 1H, t, $J = 8.6$ Hz, Ar-H), 7.42 (1H, dd, $J = 7.3, 1.3$ Hz, Ar-H), 7.80 (3H, m, Ar-H); FABMS m/z : 586 [M + H]⁺.

11-(4-Fluoro-3-methylbenzoyl)kobusine (16a). 25% yield; colorless amorphous solid; HR-FABMS m/z : 450.2439 [M + H]⁺ calcd for C₂₈H₃₃FNO₃, 450.2444; IR (ATR) ν_{\max} cm⁻¹: 3456, 2928, 2870, 1709, 1593, 1231, 1115, 1034, 957; ¹H NMR (CDCl₃): δ 0.97 (3H, s, 18-CH₃), 2.29 (3H, d, $J = 1.8$ Hz, Ar-CH₃), 3.99 (1H, d, $J = 7.7$ Hz, 15-H), 5.07 and 5.25 (each 1H, s, C=CH₂), 5.35 (1H, d, $J = 4.6$ Hz, 11-H), 7.02 (1H, t, $J = 8.6$ Hz, Ar-H), 7.75 (1H, m, Ar-H), 7.81 (1H, dd, $J = 7.2, 1.3$ Hz, Ar-H). FABMS m/z : 450 [M + H]⁺.

11,15-Di-(3-chloro-4-fluorobenzoyl)kobusine (17). 58% yield; colorless amorphous solid; HR-FABMS m/z : 626.1689 [M + H]⁺ calcd for C₃₄H₃₂Cl₂F₂NO₄, 626.1676; IR (ATR) ν_{\max} cm⁻¹: 2932, 2866, 1717, 1597, 1227, 1103, 1061, 957; ¹H NMR (CDCl₃): δ 0.96 (3H, s, 18-CH₃), 5.15 and 5.36 (each 1H, s, C=CH₂), 5.46 (1H, d, $J = 5.0$ Hz, 11-H), 5.77 (1H, s, 15-H), 7.01 and 7.06 (each 1H, t, $J = 8.6$ Hz, Ar-H), 7.85 (2H, m, Ar-H), 7.90 and 7.96 (each 1H, dd, $J = 7.2, 2.3$ Hz, Ar-H); FABMS m/z : 630 [M + 4 + H]⁺, 628 [M + 2 + H]⁺, 626 [M + H]⁺.

11,15-Di-(2,4,5-trifluoro-3-methoxybenzoyl)kobusine (18). 55% yield; colorless oil; HR-FABMS m/z : 690.2303 [M + H]⁺ calcd for C₃₆H₃₄F₆NO₆, 690.2290; IR (ATR) ν_{\max} cm⁻¹: 2943, 2870, 1717, 1620, 1234, 1103, 1057, 957; ¹H NMR (CDCl₃): δ 0.97 (3H, s, 18-CH₃), 3.94 and 3.95 (each 3H, s, Ar-OCH₃), 5.14 and 5.38 (each 1H, s, C=CH₂), 5.40 (1H, d, $J = 5.0$ Hz, 11-H), 5.73 (1H, s, 15-H), 7.29 and 7.42 (each 1H, ddd, $J = 10.4, 8.6, 6.4$ Hz, Ar-H); FABMS m/z : 690 [M + H]⁺.

11-(2,4,5-Trifluoro-3-methoxybenzoyl)kobusine (18a). 19% yield; colorless amorphous solid; HR-FABMS m/z : 502.2200 [M + H]⁺ calcd for C₂₈H₃₁F₃NO₄, 502.2205; IR (ATR) ν_{\max} cm⁻¹: 3391, 2932, 2859, 1724, 1223, 1103, 1057, 945; ¹H NMR (CDCl₃): δ 0.99 (3H, s, 18-CH₃), 3.98 (1H, s, 15-H), 4.04 (3H, s, Ar-OCH₃), 5.05 and 5.26 (each 1H, s, C=CH₂), 5.41 (1H, d, $J = 4.9$ Hz, 11-H), 7.48 (1H, ddd, $J = 10.4, 8.6, 6.4$ Hz, Ar-H); FABMS m/z : 502 [M + H]⁺.

11,15-Di-(2,3,4,5,6-pentafluorobenzoyl)kobusine (19). 26% yield; dark-brown oil; HR-EIMS m/z : 701.1597 [M]⁺ calcd for C₃₄H₂₅F₁₀NO₄, 701.1624; IR (ATR) ν_{\max} cm⁻¹: 2931, 2870, 1728, 1651, 1523, 1497, 1330, 1227, 995; ¹H NMR (CDCl₃): δ 1.00 (3H, s, 18-CH₃), 5.16 and 5.35 (each 1H, s, C=CH₂), 5.43 (1H, d, $J = 4.5$ Hz, 11-H), 5.75 (1H, s, 15-H); EIMS m/z : 701 [M]⁺, 506 [M - COC₆F₅]⁺, 195 [COC₆F₅]⁺.

11,15-Di-(2-chlorobenzoyl)kobusine (20). 59% yield; colorless amorphous solid; HR-EIMS m/z : 589.1797 [M]⁺ calcd for C₃₄H₃₃Cl₂NO₄, 589.1787; IR (ATR) ν_{\max} cm⁻¹: 2931, 2870, 2843, 1721, 1589, 1246, 1119, 1045; ¹H NMR (CDCl₃): δ 0.97 (3H, s, 18-CH₃), 5.13 and 5.36 (each 1H, s, C=CH₂), 5.42 (1H, d, $J = 4.5$ Hz, 11-H), 5.81 (1H, s, 15-H), 6.74, 7.06, 7.27, and 7.36 (each 1H, t, $J = 7.7$ Hz, Ar-H), 7.37, 7.40, 7.67, and 7.69 (each 1H, d, $J = 7.7$ Hz, Ar-H); EIMS m/z : 593 [M + 4]⁺, 591 [M + 2]⁺, 589 [M]⁺, 450 [M - COC₆H₄Cl]⁺, 141 [COC₆H₄Cl + 2]⁺, 139 [COC₆H₄Cl]⁺.

11,15-Di-(3-chlorobenzoyl)kobusine (21). 69% yield; colorless oil; HR-EIMS m/z : 589.1767 [M]⁺ calcd for C₃₄H₃₃Cl₂NO₄, 589.1787; IR (ATR) ν_{\max} cm⁻¹: 2931, 2866, 2847, 1713, 1574, 1250, 1126, 1072; ¹H NMR (CDCl₃): δ 0.96 (3H, s, 18-CH₃), 5.14 and 5.36 (each 1H, s, C=CH₂),

5.47 (1H, d, $J = 4.9$ Hz, 11-H), 5.79 (1H, s, 15-H), 7.15 and 7.20 (each 1H, t, $J = 8.2$ Hz, Ar-H), 7.42 and 7.46 (each 1H, d, $J = 8.2$ Hz, Ar-H), 7.81 (2H, d, $J = 8.2$ Hz, Ar-H), 7.88 and 7.90 (each 1H, s, Ar-H); EIMS m/z : 593 [M + 4]⁺, 591 [M + 2]⁺, 589 [M]⁺, 450 [M - COC₆H₄Cl]⁺, 141 [COC₆H₄Cl + 2]⁺, 139 [COC₆H₄Cl]⁺.

11,15-Di-(4-chlorobenzoyl)kobusine (22). 28% yield; colorless amorphous solid; HR-EIMS m/z : 589.1797 [M]⁺ calcd for C₃₄H₃₃Cl₂NO₄, 589.1787; IR (ATR) ν_{\max} cm⁻¹: 2936, 2866, 2847, 1713, 1593, 1261, 1119, 1092; ¹H NMR (CDCl₃): δ 0.97 (3H, s, 18-CH₃), 5.14 and 5.36 (each 1H, s, C=CH₂), 5.45 (1H, d, $J = 4.9$ Hz, 11-H), 5.76 (1H, s, 15-H), 7.18, 7.21, 7.84, and 7.86 (each 2H, dt, $J = 8.6, 1.8$ Hz, Ar-H); EIMS m/z : 593 [M + 4]⁺, 591 [M + 2]⁺, 589 [M]⁺, 450 [M - COC₆H₄Cl]⁺, 141 [COC₆H₄Cl + 2]⁺, 139 [COC₆H₄Cl]⁺.

11,15-Di-(3,5-dichlorobenzoyl)kobusine (23). 75% yield; colorless oil; HR-EIMS m/z : 657.0984 [M]⁺ calcd for C₃₄H₃₁Cl₄NO₄, 657.1007; IR (ATR) ν_{\max} cm⁻¹: 2928, 2866, 1717, 1570, 1254, 1146, 1099; ¹H NMR (CDCl₃): δ 0.97 (3H, s, 18-CH₃), 5.17 and 5.40 (each 1H, s, C=CH₂), 5.47 (1H, d, $J = 5.0$ Hz, 11-H), 5.77 (1H, s, 15-H), 7.43 and 7.46 (each 1H, t, $J = 1.8$ Hz, Ar-H), 7.72 and 7.74 (each 2H, d, $J = 1.8$ Hz, Ar-H); EIMS m/z : 667 [M + 8]⁺, 665 [M + 6]⁺, 661 [M + 4]⁺, 659 [M + 2]⁺, 657 [M]⁺, 484 [M - COC₆H₃Cl₂]⁺, 175 [COC₆H₃Cl₂ + 2]⁺, 173 [COC₆H₃Cl₂]⁺.

11-(3,5-Dichlorobenzoyl)kobusine (23a). 10% yield; colorless amorphous solid; HR-EIMS m/z : 485.1518 [M]⁺ calcd for C₂₇H₂₉Cl₂NO₃, 485.1524; IR (ATR) ν_{\max} cm⁻¹: 2970, 2936, 1738, 1570, 1215; ¹H NMR (CDCl₃): δ 0.99 (3H, s, 18-CH₃), 4.03 (1H, s, 15-H), 5.08 and 5.26 (each 1H, s, C=CH₂), 5.35 (1H, d, $J = 4.5$ Hz, 11-H), 7.53 (1H, t, $J = 1.8$ Hz, Ar-H), 7.81 (2H, d, $J = 1.8$ Hz, Ar-H); EIMS m/z : 489 [M + 4]⁺, 487 [M + 2]⁺, 485 [M]⁺, 312 [M - COC₆H₃Cl₂]⁺, 173 [COC₆H₃Cl₂]⁺.

11,15-Di-(4-chloro-3-nitrobenzoyl)kobusine (24). 11% yield; colorless amorphous solid; HR-FABMS m/z : 680.1559 [M + H]⁺ calcd for C₃₄H₃₂Cl₂N₃O₈, 680.1566; IR (ATR) ν_{\max} cm⁻¹: 2924, 2856, 1717, 1605, 1535, 1242, 1103, 1049, 957; ¹H NMR (CDCl₃): δ 0.98 (3H, s, 18-CH₃), 5.17 and 5.38 (each 1H, s, C=CH₂), 5.50 (1H, d, $J = 4.5$ Hz, 11-H), 5.81 (1H, s, 15-H), 7.51 and 7.56 (each 1H, d, $J = 8.2$ Hz, Ar-H), 8.06 and 8.08 (each 1H, dd, $J = 8.2, 1.8$ Hz, Ar-H), 8.22 and 8.29 (each 1H, d, $J = 1.8$ Hz, Ar-H); FABMS m/z : 684 [M + 4 + H]⁺, 682 [M + 2 + H]⁺, 680 [M + H]⁺.

11,15-Di-(4-dichloromethylbenzoyl)kobusine (25). 62% yield; colorless amorphous solid; HR-FABMS m/z : 686.1404 [M + H]⁺ calcd for C₃₆H₃₆Cl₄NO₄, 686.1398; IR (ATR) ν_{\max} cm⁻¹: 2924, 2855, 1713, 1612, 1582, 1231, 1107, 1018, 953; ¹H NMR (CDCl₃): δ 0.96 (3H, s, 18-CH₃), 5.14 and 5.34 (each 1H, s, C=CH₂), 5.47 (1H, d, $J = 4.5$ Hz, 11-H), 5.79 (1H, s, 15-H), 6.63 and 6.65 (each 1H, s, Ar-CHCl₂), 7.41, 7.42, 7.95, and 7.99 (each 1H, d, $J = 8.6$ Hz, Ar-H); FABMS m/z : 694 [M + 8 + H]⁺, 692 [M + 6 + H]⁺, 690 [M + 4 + H]⁺, 688 [M + 2 + H]⁺, 686 [M + H]⁺.

Cell Culture, Cytotoxicity, and Cell Cycle Analysis. All cell lines used in this study were obtained from American Type Culture Collection (ATCC, Virginia, USA) or UNC Lineberger Comprehensive Cancer Center (North Carolina, USA), except KB-VIN (MDR subline established from KB), which was provided by Professor Y.-C. Cheng (Yale University, Connecticut, USA). All cell lines were cultured in RPMI 1640 medium containing 25 mM HEPES and 2 mM L-glutamine (Corning, New York, USA), supplemented with 10% fetal

bovine serum (Sigma-Aldrich, Missouri, USA), 100 $\mu\text{g}/\text{mL}$ streptomycin, 100 IU penicillin, and 0.25 $\mu\text{g}/\text{mL}$ amphotericin B (Corning, New York, USA). KB-VIN were maintained in a medium containing 100 nM vincristine (Sigma-Aldrich, Missouri, USA). Cells were cultured at 37 °C in a humidified 5% CO_2 atmosphere.

Antiproliferative activity was assessed by the sulforhodamine B (SRB) method as described before.²⁵ Briefly, all derivatives were prepared at 10 mM with DMSO, and the highest DMSO concentration in the cultures (0.4% v/v) used for the antiproliferative activity assay had no effect on cell growth. Freshly trypsinized cell suspensions were seeded in 96-well microtiter plates at densities of 4000–11,000 cells per well with derivatives for 72 h, followed by fixation in 10% trichloroacetic acid and then staining with 0.04% SRB. The protein-bound dye was solubilized by 10 mM Tris base, and the absorbance was measured at 515 nm using a ELx800 microplate reader operated by Gen5 software (BioTek, Vermont, USA). The IC_{50} value was calculated from at least three independent experiments performed in duplicate.

MDA-MB-231 (1×10^5 cells/well) cells were seeded in a 12-well plate 24 h prior to treatment with derivatives. After 12 or 24 h treatment with derivatives at a concentration 3-fold of their IC_{50} value ($3 \times \text{IC}_{50}$), cells were harvested and fixed with 70% EtOH, followed by staining with PI containing RNase (BD Bioscience). Stained cells were analyzed using a flow cytometer (BD LSRIL, BD Biosciences). 200 nM CA-4 was used as tubulin polymerization inhibitor arresting cells in G2/M.

■ ASSOCIATED CONTENT

SI Supporting Information

The Supporting Information is available free of charge at <https://pubs.acs.org/doi/10.1021/acsomega.2c02363>.

¹H NMR spectra for derivatives **4**, **5**, **7–9**, **7a–9a**, **7b**, **9b**, **13**, **13a**, **16–25**, **16a**, **18a**, and **23a** (PDF)

■ AUTHOR INFORMATION

Corresponding Author

Koji Wada – Department of Medicinal Chemistry, Faculty of Pharmaceutical Sciences, Hokkaido University of Science, Sapporo 006-8585, Japan; orcid.org/0000-0002-6064-0996; Email: kowada@hus.ac.jp

Authors

Masuo Goto – Division of Chemical Biology and Medicinal Chemistry, UNC Eshelman School of Pharmacy, University of North Carolina, Chapel Hill, North Carolina 27599-7568, United States; orcid.org/0000-0002-9659-1460

Hisano Tanaka – Department of Medicinal Chemistry, Faculty of Pharmaceutical Sciences, Hokkaido University of Science, Sapporo 006-8585, Japan

Megumi Mizukami – Department of Medicinal Chemistry, Faculty of Pharmaceutical Sciences, Hokkaido University of Science, Sapporo 006-8585, Japan

Yuji Suzuki – Department of Medicinal Chemistry, Faculty of Pharmaceutical Sciences, Hokkaido University of Science, Sapporo 006-8585, Japan

Kuo-Hsiung Lee – Division of Chemical Biology and Medicinal Chemistry, UNC Eshelman School of Pharmacy, University of North Carolina, Chapel Hill, North Carolina

27599-7568, United States; orcid.org/0000-0002-6562-0070

Hiroshi Yamashita – Department of Medicinal Chemistry, Faculty of Pharmaceutical Sciences, Hokkaido University of Science, Sapporo 006-8585, Japan

Complete contact information is available at:

<https://pubs.acs.org/10.1021/acsomega.2c02363>

Author Contributions

[§]K.W. and M.G. contributed equally to this work.

Notes

The authors declare no competing financial interest.

■ ACKNOWLEDGMENTS

We thank Dr. Susan L. Morris-Natschke (UNC-CH) for critical comments, suggestions, and editing of the manuscript. This study was supported in part by a Grant-in-Aid (2021) provided by Hokkaido University of Science to K.W. and by NIH grant CA177584 from the National Cancer Institute awarded to K.H.L. as well as IBM junior faculty development grant awarded to M.G.

■ REFERENCES

- (1) Newman, D. J.; Cragg, G. M. Natural products as sources of new drugs over the nearly four decades from 01/1981 to 09/2019. *J. Nat. Prod.* **2020**, *83*, 770–803.
- (2) Haveman, J.; Castro Kreder, N.; Rodermond, H. M.; Van Bree, C.; Franken, N. A.; Stalpers, L. J.; Zdzienicka, M. Z.; Peters, G. J. Cellular response of X-ray sensitive hamster mutant cell lines to gemcitabine, cisplatin and 5-fluorouracil. *Oncol. Rep.* **2004**, *12*, 187–192.
- (3) Diedelot, C.; Mirjolet, J. F.; Barberi-Heyob, M. Radiation could induce p53-independent and cell cycle-unrelated apoptosis in 5-fluorouracil radiosensitized head and neck carcinoma cells. *Can. J. Physiol. Pharmacol.* **2002**, *80*, 638–643.
- (4) Pauwels, B.; Korst, A. E. C.; Andriessen, V.; Baay, M. F. D.; Pattyn, G. G. O.; Lambrechts, H. A. J.; Pooter, C. M. J.; Lardon, F.; Vermorken, J. B. Unraveling the mechanism of radiosensitization by gemcitabine: the role of TP53. *Radiat. Res.* **2005**, *164*, 642–650.
- (5) Zhang, M.; Boyer, M.; Rivory, L.; Hong, A.; Clarke, S.; Stevens, G.; Fife, K. Radiosensitization of vinorelbine and gemcitabine in NCL-H460 non-small-cell lung cancer cell. *Int. J. Radiat. Oncol., Biol., Phys.* **2004**, *58*, 353–360.
- (6) Baumann, M.; Krause, M. Targeting the epidermal growth factor receptor in radiotherapy: radiobiological mechanisms, preclinical and clinical results. *Radiother. Oncol.* **2004**, *72*, 257–266.
- (7) Kvols, L. K. Radiation sensitizers: a selective review of molecules targeting DNA and non-DNA targets. *J. Nucl. Med.* **2005**, *46*, 187S–190S.
- (8) Sonnemann, J.; Gekeler, V.; Ahlbrecht, K.; Brischwein, K.; Liu, C.; Bader, P.; Müller, C.; Niethammer, D.; Beck, J. F. Down-regulation of protein kinase C η by antisense oligonucleotides sensitizes A549 lung cancer cells to vincristine and paclitaxel. *Cancer Lett.* **2004**, *209*, 177.
- (9) Qing, C.; Jiang, C.; Zhang, J. S.; Ding, J. Induction of apoptosis in human leukemia K-562 and gastric carcinoma SGC-7901 cells by salvicine, a novel anticancer compound. *Anticancer Drugs* **2001**, *12*, 51–56.
- (10) Meng, L. H.; Zhang, J. S.; Ding, J. Salvicine, a novel DNA topoisomerase II inhibitor, exerting its effects by trapping enzyme-DNA cleavage complexes. *Biochem. Pharmacol.* **2001**, *62*, 733–741.
- (11) Amiya, T.; Bando, H. *Aconitum* alkaloids. *The Alkaloids*; Brossi, A., Ed.; Academic Press: San Diego, 1988; Vol. 34, pp 95–179.
- (12) Wang, F. P.; Chen, Q. H. The C₁₉-Diterpenoid Alkaloids. *The Alkaloids: Chemistry and Biology*; Cordell, G. A., Ed.; Academic Press: San Diego, 2010; Vol. 69, pp 1–577.

(13) Benn, M. H.; Jacyno, J. M. The toxicology and pharmacology of diterpenoid alkaloids. *Alkaloids: Chemical and Biological Perspectives*; Pelletier, S. W., Ed.; Wiley-Interscience: New York, 1983; Vol. 1, pp 153–210.

(14) Wada, K.; Hazawa, M.; Takahashi, K.; Mori, T.; Kawahara, N.; Kashiwakura, I. Inhibitory effects of diterpenoid alkaloids on the growth of A172 human malignant cells. *J. Nat. Prod.* **2007**, *70*, 1854–1858.

(15) Hazawa, M.; Wada, K.; Takahashi, K.; Mori, T.; Kawahara, N.; Kashiwakura, I. Suppressive effects of novel derivatives prepared from *Aconitum* alkaloids on tumor growth. *Invest. New Drugs* **2009**, *27*, 111–119.

(16) Hazawa, M.; Takahashi, K.; Wada, K.; Mori, T.; Kawahara, N.; Kashiwakura, I. Structure–activity relationships between the *Aconitum* C₂₀-diterpenoid alkaloid derivatives and the growth suppressive activities of Non-Hodgkin's lymphoma Raji cells and human hematopoietic stem/progenitor cells. *Invest. New Drugs* **2011**, *29*, 1–8.

(17) Wada, K.; Hazawa, M.; Takahashi, K.; Mori, T.; Kawahara, N.; Kashiwakura, I. Structure-activity relationships and the cytotoxic effects of novel diterpenoid alkaloid derivatives against A549 human lung carcinoma cells. *J. Nat. Med.* **2011**, *65*, 43–49.

(18) Wada, K.; Ohkoshi, E.; Bastow, K. F.; Morris-Natschke, S. L.; Lee, K. H. Cytotoxic esterified diterpenoid alkaloid derivatives with increased selectivity against a drug-resistant cancer cell line. *Bioorg. Med. Chem. Lett.* **2012**, *22*, 249–252.

(19) Wada, K.; Ohkoshi, E.; Zhao, Y.; Goto, M.; Morris-Natschke, S. L.; Lee, K. H. Evaluation of *Aconitum* diterpenoid alkaloids as antiproliferative agents. *Bioorg. Med. Chem. Lett.* **2015**, *25*, 1525–1531.

(20) Wada, K.; Goto, M.; Shimizu, T.; Kusanagi, N.; Mizukami, K. P.; Suzuki, K. H.; Li, H.; Lee, K.-H.; Yamashita, H. Structure-activity relationships and evaluation of esterified diterpenoid alkaloid derivatives as antiproliferative agents. *J. Nat. Med.* **2019**, *73*, 789–799.

(21) Wada, K.; Bando, H.; Amiya, T. Two new C₂₀-diterpenoid alkaloids from *Aconitum yesoense* var. *macroyesoense* (NAKAI) TAMURA. Structures of dehydrolucidusculine and *N*-deethyldehydrolucidusculine. *Heterocycles* **1985**, *23*, 2473–2477.

(22) Wada, K.; Kawahara, N. Diterpenoid and norditerpenoid alkaloids from the roots of *Aconitum yesoense* var. *macroyesoense*. *Helv. Chim. Acta* **2009**, *92*, 629–637.

(23) Wada, K.; Ishizuki, S.; Mori, T.; Fujihira, E.; Kawahara, N. Effects of *Aconitum* alkaloid kobusine and pseudokobusine derivatives on cutaneous blood flow in mice. *Biol. Pharm. Bull.* **1998**, *21*, 140–146.

(24) Wada, K.; Ishizuki, S.; Mori, T.; Fujihira, E.; Kawahara, N. Effects of *Aconitum* alkaloid kobusine and pseudokobusine derivatives on cutaneous blood flow in mice; II. *Biol. Pharm. Bull.* **2000**, *23*, 607–615.

(25) Nakagawa-Goto, K.; Oda, A.; Hamel, E.; Ohkoshi, E.; Lee, K. H.; Goto, M. Development of a novel class of tubulin inhibitor from desmosdumotin B with a hydroxylated bicyclic B-ring. *J. Med. Chem.* **2015**, *58*, 2378–2389.